Proceedings of the 12th World Congress on Electrical Engineering and Computer Systems and Sciences (EECSS'25)
Paris, France – August 17 - 19, 2025
Paper No. ICBES 134
DOI: 10.11159/icbes25.134

Robotic Laser Microscope Systems for Tissue-Level Investigation: Applications in Collagen and Drosophila Brain Tissues

Jiayu Hu*, Sophia Liu*, Xuning Ye*, Rehaan Hassan*, Huiying Huang, Zachary Wang, Veronica Gomez-Godinez, Linda Shi†[2]
[1]Institute of Engineering in Medicine, University of California San Diego, La Jolla, CA, 92093
† Correspondence: zshi@ucsd.edu
*High school students participating in IEM OPALS program

Abstract **–** Short pulsed Laser-induced microscope systems present a powerful tool for inducing precise and localized damage in live cells to investigate fundamental biomechanics and cellular response pathways. Traditionally applied to live-cell damage in research areas such as DNA repair, cellular biomechanics, chromatin structure during mitosis, and mitotic checkpoint regulation, and neurodegenerative diseases, we explore the application of two platforms—femtosecond laser ablation and laser-induced shockwaves (LIS)—for analysing on tissue level changes in collagen fibers and brain tissues from Drosophila. Our collagen fiber study demonstrates a measurable 30% increase in tissue thickness surrounding the ablation zone, captured using quantitative phase imaging (QPI). Concurrently, LIS investigation of fly brain morphology reveals that total volume, rather than shape, determines resistance to mechanical shock. These studies reinforce the adaptability of laser-induced microscope systems across biological scales, highlighting their application in tissue engineering, neurodegenerative diseases, and regenerative medicine.

Keywords**:** Laser-induced Shockwave, Femtosecond Pulsed Laser Ablation, Robotic Laser Microscope Systems, Collagen Tissue, Drosophila Brain Tissue

1. Introduction

Laser-induced microscope systems have become vital instruments in biomedical engineering, offering non-contact, high-precision tools for manipulating biological materials at both cellular and subcellular scales. These systems enable researchers to probe the mechanical and biochemical properties of cells with exceptional spatial and temporal resolution, unlocking new frontiers in diagnostics, regenerative medicine, and mechanobiology. In particular, the therapeutic potential of photonic interventions—such as photobiomodulation, laser ablation, and shockwave-based therapies—has been extensively demonstrated in preclinical and translational studies.

Photobiomodulation, for example, has been shown to modulate microbiota-related dysbiosis [1], accelerate tendon healing [2], and promote angiogenesis in ischemic tissues [3]. Low-level laser therapy also enhances osteogenic differentiation and mineralization in human dental pulp stem cells and modulates macrophage behavior during bone remodeling [4,5]. In parallel, laser-based technologies have been adapted for oncologic therapies—such as curcumin-gold nanoshells combined with near-infrared irradiation to selectively target ovarian cancer cells [6]—and for molecular-level diagnostics using Raman spectroscopy to assess intracellular photobiomodulation effects [7].

Building on this growing body of evidence, our laboratory has spent over two decade advancing robotic laser microscope systems that integrate femtosecond laser ablation and laser-induced shockwave (LIS) modalities. These platforms have powered numerous studies in nuclear DNA damage repair [8], chromatin structure during mitosis [9], and degenerative disease models including Huntington's and Charcot-Marie-Tooth neuropathies [10,11]. LIS has also proven effective in modeling axonal injury and eliciting neuronal calcium responses in real time, allowing us to study neural mechanotransduction under physiologically relevant conditions [12].

A cornerstone of our research has been the development of a metasurface-based quantitative phase imaging (QPI) system, inspired by the compound eye structure of birds, which permits real-time, label-free imaging of nanoscale morphological changes in tissue [13]. This system has been successfully coupled with deep learning-enhanced image reconstruction and has expanded our ability to monitor mechanical perturbations in live biological samples with minimal photodamage.

Here, we extended the application of these robotic laser microscope systems to tissue-level studies for the first time. Specifically, we investigated the morphological responses of bovine collagen fibers following femtosecond laser ablation and dissected Drosophila melanogaster brain tissues following LIS. By combining QPI and phase contrast imaging, we quantified post-ablation collagen remodeling and evaluated how brain tissue geometry affected its resistance to mechanical deformation. The findings presented in this study not only affirm the scalability and precision of our laser platforms but also open new avenues for tissue engineering, neuroengineering, and laser-assisted diagnostics and therapeutics.

2. Materials and Methods

2.1 Collagen Tissue Ablation and Quantitative Phase Imaging

To investigate the structural response of connective tissue under precise localized laser damage, bovine Achilles tendon collagen fibers were harvested and manually dissected into thin, parallel bundles. Samples were maintained in phosphate-buffered saline (PBS) during imaging to preserve physiological conditions.

Femtosecond laser ablation was performed using a Ti:Sapphire Mai Tai laser (Spectra-Physics) operating at 780 nm, pulse width <100 fs, and repetition rate of 80 MHz. The laser beam was directed through a high-numerical-aperture (NA) objective lens and focused onto a localized 1.12 μm-wide region of the collagen matrix. Energy levels were optimized to minimize collateral damage beyond the target ablation site, following protocols similar to those used in subnuclear chromatin dissection and interstrand crosslinking repair studies [8].

High-resolution pre- and post-ablation images were collected using QuantEM (Photometrics), and the thickness images using the FOSSMM (Fourier Optics-based Scattering Sensing Metasurface Microscopy) platform[12]. This custom system, developed in collaboration with the Liu labs, integrates metasurface optics inspired by the compound eyes of eagles to produce enhanced quantitative phase imaging (QPI). QPI enables label-free, non-contact visualization of nanoscale refractive index variations in biological samples and was enhanced here by a deep learning-assisted image reconstruction algorithm trained on synthetic and experimental data. Amplitude and phase images were reconstructed to assess changes in fiber thickness and morphology surrounding the ablation zone.

For analysis, image stacks were registered and segmented using FIJI/ImageJ. Tissue thickness at the site of ablation was quantitatively assessed, with pre- and post-treatment averages compared using paired t-tests. QPI resolution limits (~1.12 μm) were noted, and any structures below this threshold were excluded from the final dataset.

2.2 Drosophila Brain Tissue Dissection and Laser-Induced Shockwave (LIS)

To evaluate the biomechanical properties of brain tissue under mechanical stress, Drosophila melanogaster (fruit fly) brains were dissected. Brains were harvested in cold dissection buffer under a dissection microscope (Olympus LUCPlanFL) and immediately incubated in a staining solution containing Hoechst 33342 (5 μg/mL, Thermo Fisher) for nuclear labeling and Ethidium Homodimer-1 (EthD-1, 4 μM) to identify compromised cell membranes. Tissues were placed in the petri dish (35 mm Dish | No. 1.5 Coverslip, MatTek) throughout laser exposure.

For LIS stimulation, we employed a Coherent Flare laser system (Spectra-Physics) operating at a wavelength of 1032 nm, with a 100 Hz repetition rate and a pulse width of 2 ns. Laser power was precisely modulated using a rotating optical polarizer mounted on a stepper-motor-controlled rotation stage (Newport). A mechanical shutter (Vincent Associates), configured with a 10–15 ms duty cycle, was synchronized to permit the passage of 1–2 laser pulses per activation cycle.

Beam expanders were incorporated into the optical path to match the laser beam diameter with the back aperture of the objective lens, ensuring optimal beam focusing. The laser was introduced into the microscope setup via a custom-designed laser entry port (CLEP), positioned beneath a 40× PH3 oil-immersion objective (Zeiss Phase III, NA 1.3) mounted on a Zeiss Axiovert 200M inverted microscope. The CLEP's internal filter was selected to precisely direct the laser pulses to the lower-right quadrant of the imaging field, maintaining accurate targeting within the specimen plane.

The petri dish containing the live brain tissue maintained in the stage incubator (37°C and 5% CO_2). Time-lapse imaging was performed using ORCA-Flash4.0 V2 Digital Hamamatsu CMOS camera. Imaging was conducted before, and post-shockwave to assess the brain tissue responses.

3. Results and Discussion

The present study marks the first successful application of our robotic laser microscope systems—previously validated in cellular models—to tissue-level biological samples: Our system uses the femtosecond laser ablation and the other uses laser-induced shockwave (LIS) technologies, allowing us to investigate the biomechanical properties of collagen fiber networks and the morphodynamic behavior of dissected Drosophila brain tissue under stress. The observations made in these models underscore the high-resolution capability, mechanical precision, and scalability of our system in probing tissue responses to external perturbation.

3.1 Collagen Tissue Response and Structural Remodeling

In our collagen fiber ablation experiments, we applied femtosecond laser pulses to isolated collagen bundles and visualized the structural response using QuantEM camera and metasurface-based quantitative phase imaging (QPI) system, FOSSMM. This Eagle-Eye-inspired optical platform leverages polarized light separation and solves the Transport of Intensity Equation (TIE) to generate label-free, high-resolution thickness maps. Our analysis revealed a consistent and statistically significant post-ablation increase in collagen tissue thickness—from an average of 7.78 μm to 10.68 μm, marking a 30% rise.

As illustrated in **Figure 1**, panels (a) and (b) show quantitative phase images of collagen fibers imaged via QuantEM camera before and after ablation. Panels (c) and (d) are the quantitative phase images taken of the area indicated by the green dashed frames, and Panels (e) & (f) are the topological views of (c) & (d) respectively, clearly demonstrating the thickening of the tissue post-ablation. This remodeling may reflect laser-induced thermal denaturation, fiber swelling, or partial disruption of collagen crosslinks, triggering localized structural reorganization.

The use of QPI allowed real-time monitoring without staining or destructive preparation, underscoring the platform's potential for in situ diagnostics of fibrotic remodeling, wound healing, and laser-tissue interactions. While the system achieved excellent spatial accuracy, it was unable to resolve fine structural features under 1.12 μm—such as the narrow ablation line—highlighting the current resolution limit of the system.

Future iterations of this imaging platform may benefit from the integration of higher NA objectives and improved pixel-to-micron mapping to enhance its capacity for nanoscale tissue analysis. Overall, our findings demonstrate that even modest laser doses can induce robust and measurable changes in connective tissue morphology, and our system is well-positioned to monitor these changes non-invasively.

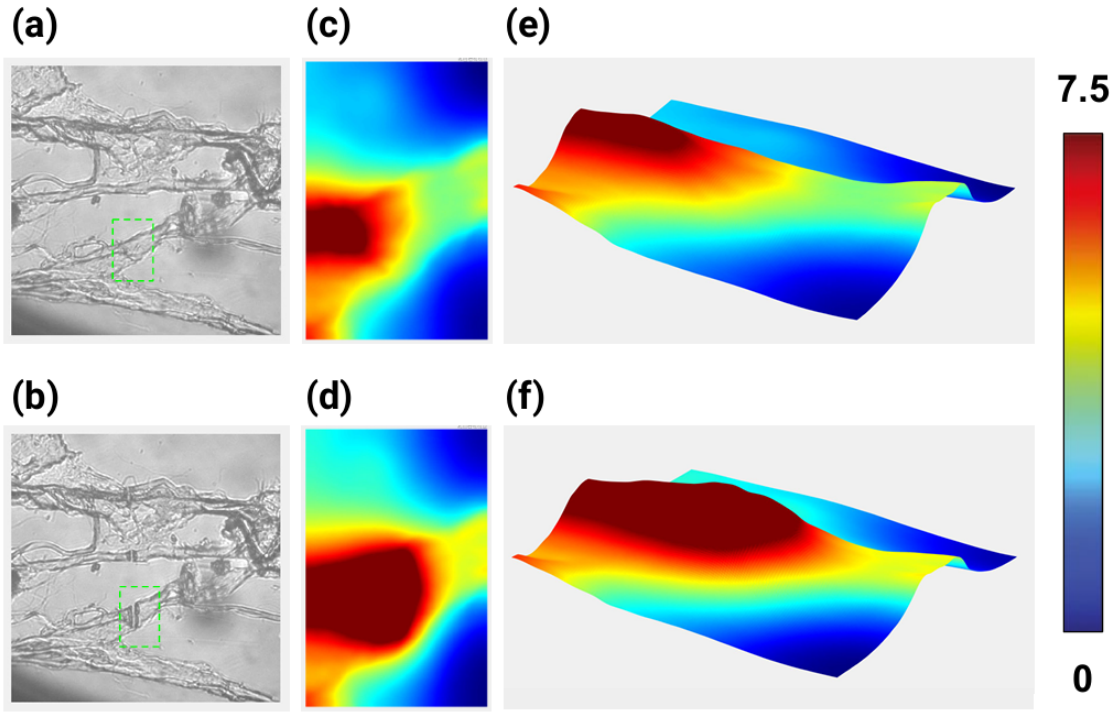

Figure 1. Structural changes in collagen tissue following laser ablation.
(a, b) Polarized camera images of collagen fibers before (a) and after (b) femtosecond laser ablation. (c, d) Corresponding quantitative phase images (QPI) generated from the yellow-dashed framed region in a and b, respectively. (e, f) Topographic reconstructions derived from phase data, showing collagen thickening post-ablation.

3.2 Drosophila Brain Tissue: Volume-Dependent Shockwave Resistance

Laser-induced shockwave (LIS) experiments conducted on dissected Drosophila brain tissues uncovered distinct biomechanical behaviors linked to tissue volume. Two structurally distinct brain types—one with a wide-flat morphology (base area = 194,132.11 μm^2) and the other with a narrow-tall structure (base area = 116,924.39 μm^2)—were subjected to sequential LIS pulses, administered at 5 µm Z-plane intervals under controlled environmental conditions.

Despite their differing geometries, both brain samples underwent comparable displacements and exhibited similar levels of apoptotic response, as indicated by EthD-1-positive fluorescence. The wide-flat brain reached full displacement after a 15 µm cumulative depth exposure, while the narrow-tall brain required a greater vertical displacement (25 µm) to achieve full shockwave effect. Volumetric analysis revealed near-identical volumes for the two morphologies: 2.91×10^6 μm^3 and 2.92×10^6 μm^3, respectively. These findings suggest that total tissue volume—not just shape or footprint—plays a dominant role in determining mechanical shock resistance.

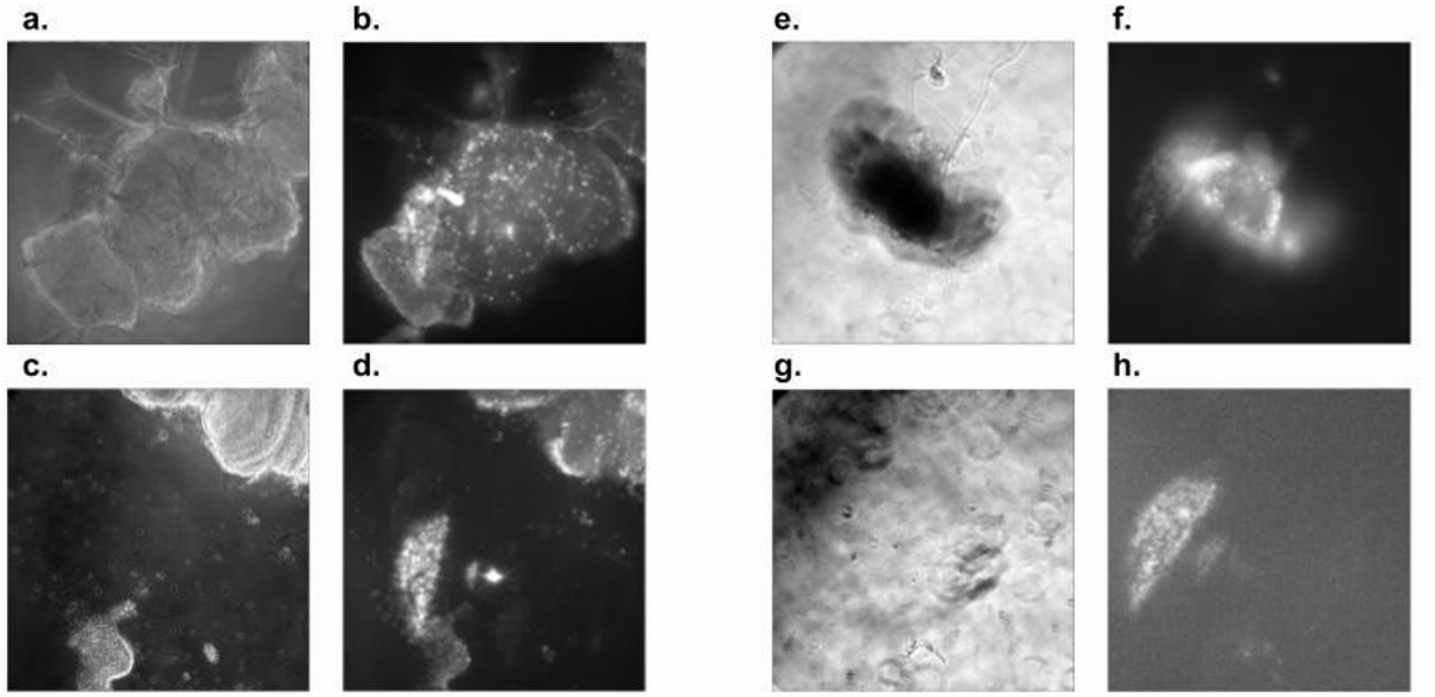

Figure 2. Comparative analysis of two morphologically distinct Drosophila brain tissues subjected to laser-induced shockwaves. (a–b) Wide-flat brain morphology at the initial focal plane captured in phase contrast and EthD-1 (Dead Red) fluorescent channels, respectively. (c–d) The same tissue after full displacement following three LIS exposures at 5 µm intervals (15 µm total), visualized in phase and fluorescence. (e–f) Narrow-tall brain morphology at the initial focal plane in phase contrast and EthD-1 channels. (g–h) Tissue post full displacement after five LIS exposures at 5 µm steps (25 µm total),

High-resolution fluorescent imaging using Hoechst 33342 and EthD-1 dyes facilitated real-time monitoring of cell nuclei and membrane-compromised cells. These results were captured and documented in **Figure 2**, which illustrated both initial focal plane images and the progressive structural displacement following LIS exposure. The consistent deformation responses observed reinforce prior findings that LIS-induced injury mechanisms were governed more by the mechanical load distribution across the tissue volume than by surface morphology alone.

This experiment, visualized in Figure 2, demonstrated the precision and efficiency of our LIS setup in targeting and assessing volume-specific tissue responses. These insights may contribute to future research on the biomechanics of traumatic brain injury (TBI) models and tissue-level damage resilience.

3.3 Broader Implications and Technological Validation

Collectively, these results validate our robotic laser microscope systems as powerful platforms for biomechanical studies at the tissue scale. The high reproducibility of the observed phenomena across replicates supports the robustness of the approach. The integration of deep learning-assisted QPI and precision LIS mechanisms extends the scope of our prior work in live-cell research and demonstrates that the same platforms can be adapted for tissue-level mechanobiology, damage simulation, and diagnostics.

This versatility opens several new research directions. First, the clear structure-function relationships uncovered in collagen and brain tissues point to future work in patient-derived organoids, engineered scaffolds, and decellularized matrices. Second, coupling our laser ablation and LIS systems with AI-based classification may accelerate the discovery of

new mechanical biomarkers. Finally, these systems may be used to simulate therapeutic perturbations for drug screening and targeted therapy in soft tissue pathologies.

4. Conclusion

This study represents a pivotal step in extending the capabilities of our robotic laser microscope systems—originally designed for cellular-level investigations—into tissue-level applications with high spatial precision and functional relevance. By integrating femtosecond laser ablation and laser-induced shockwave (LIS) technologies with advanced imaging modalities such as quantitative phase imaging (QPI) and fluorescence microscopy, we demonstrated the feasibility of applying these tools to study dynamic structural and biomechanical changes in both extracellular matrices (collagen) and complex neuronal tissues (Drosophila brain).

Our results not only confirmed the system's sensitivity in detecting morphological adaptations, such as the significant thickening of collagen fibers post-ablation but also revealed critical insights into how tissue volume governs mechanical resilience in brain models exposed to shockwave stress. The consistency in displacement patterns observed across structurally distinct brain morphologies highlights the potential universality of volume as a predictive parameter for tissue integrity under stress.

These findings offer valuable implications for multiple fields, including neuroengineering, regenerative medicine, and tissue biomechanics. The ability to induce and monitor controlled microtrauma in both soft connective tissue and neuronal architectures opens new avenues for studying injury response, cellular repair, and therapeutic intervention mechanisms. Moreover, this approach provides a versatile platform for testing biomaterials, evaluating drug candidates, and developing computational models that simulate trauma at multiple biological scales.

Future directions for this work include the integration of artificial intelligence and machine learning to automate damage classification and improve interpretation of phase and fluorescence signals. Additionally, we plan to expand the system's use in vivo, enabling longitudinal studies of injury progression and healing. Finally, further exploration into coupling our platform with optogenetic and electrophysiological readouts could significantly enhance the scope of real-time mechanobiological studies.

In conclusion, this study not only validates the tissue-level applications of our robotic laser platforms but also sets the stage for their broader use in next-generation biomedical research aimed at bridging cellular phenomena with whole-tissue physiology.

Acknowledgements

We would like to thank Dr. Lingyan Shi's lab for providing the fruit flies (Drosophila), and Dr. Wei Xiong's lab for providing the collagen samples. This material was based upon work supported by a gift from Beckman Laser Institute Inc. to LS & VGG. Special thanks to the private donors to our UCSD IEM BTC center: Dr. Shu Chien from UCSD Bioengineering, Dr. Lizhu Chen from CorDx Inc., Dr. Xinhua Zheng, David & Leslie Lee for their generous donations.

References

[1] Pourhajibagher M, Gharibpour F, Nikparto N, Bahrami R, Bahador A. The effect of photobiomodulation on oral microbiota dysbiosis: A literature review. *Photodiagnosis Photodyn Ther.* 2025 Apr;52:104525. doi: 10.1016/j.pdpdt.2025.104525. PMID: 39956443.

[2] Lim JK, Kim JH, Park GT, Woo SH, Cho M, Kang SW. Efficacy of Light-Emitting Diode-Mediated Photobiomodulation in Tendon Healing in a Murine Model. *Int J Mol Sci.* 2025 Mar 4;26(5):2286. doi: 10.3390/ijms26052286. PMID: 40076906; PMCID: PMC11899806.

[3] Sung PH, Yeh JN, Yin TC, Chai HT, Chiang JY, Huang CR, Chen YL, Lee MS, Yip HK. Extracorporeal shockwave therapy rescued mouse critical limb ischemia via upregulating GPR120 against inflammation and promoting angiogenesis for restoring the blood flow in ischemic zone—experimental study. *Int J Surg.* 2025 Mar 1;111(3):2414-2429. doi: 10.1097/JS9.0000000000002243. PMID: 39869384.

[4] Yoshida R, Kobayashi K, Onuma K, Yamamoto R, Chiba-Ohkuma R, Karakida T, Yamakawa S, Hosoya N, Yamazaki Y, Yamakoshi Y. Enhancement of differentiation and mineralization of human dental pulp stem cells via TGF-β signaling in low-level laser therapy using Er:YAG lasers. *J Oral Biosci.* 2025 Mar;67(1):100617. doi: 10.1016/j.job.2025.100617. PMID: 39832694.

[5] Mayahara K, Okuma R, Sasagawa T, Motoyoshi M, Shimizu N. Effects of low-level laser irradiation on osteoclastogenesis in prostaglandin E2-stimulated macrophages. *Lasers Med Sci.* 2025 Mar 28;40(1):163. doi: 10.1007/s10103-025-04423-w. PMID: 40153082.

[6] Rokhgireh S, Chaichian S, Mehdizadeh Kashi A, Haji Ali B, Tehermanesh K, Ajdary M, Nasir S, Pirhajati Mahabadi V, Eslahi N. Curcumin-gold nanoshell mediated near-infrared irradiation on human ovarian cancer cell: in vitro study. *Med Oncol.* 2025 Apr 1;42(5):145. doi: 10.1007/s12032-025-02687-4. PMID: 40167850.

[7] Rastogi M, Chowdhury A, Chakraborty S, Sahu K, Majumder SK. Label-free and real-time assessment of 660 nm red light photobiomodulation induced molecular alterations in human adipose-derived mesenchymal stem cells using micro Raman spectroscopy. *Spectrochim Acta A Mol Biomol Spectrosc.* 2025 Mar 15;329:125552. doi: 10.1016/j.saa.2024.125552. PMID: 39647267.

[8] Duquette ML, Zhu Q, Taylor ER, Tsay AJ, Shi LZ, Berns MW, McGowan CH. CtIP is required to initiate replication-dependent interstrand crosslink repair. *PLoS Genet.* 2012;8(11):e1003050. doi: 10.1371/journal.pgen.1003050. PMID: 23144634; PMCID: PMC3493458.

[9] Shah SB, Li Y, Li S, Hu Q, Wu T, Shi Y, Nguyen T, Ive I, Shi L, Wang H, Wu X. 53BP1 deficiency leads to hyperrecombination using break-induced replication (BIR). *Nat Commun.* 2024;15(1):8648. doi: 10.1038/s41467-024-52916-z. PMID: 39368985; PMCID: PMC11455893.

[10] Barber S, Gomez-Godinez V, Young J, Wei A, Chen S, Snissarenko A, Chan SS, Wu C, Shi L. Impacts of H2O2, SARM1 inhibition, and high NAm concentrations on Huntington's disease laser-induced degeneration. *J Biophotonics.* 2024;17(3):e202300370. doi: 10.1002/jbio.202300370.

[11] Gu Y, Guerra F, Hu M, Pope A, Sung K, Yang W, Jetha S, Shoff TA, Gunatilake T, Dahlkamp O, Shi LZ, Manganelli F, Nolano M, Zhou Y, Ding J, Bucci C, Wu C. Mitochondria dysfunction in Charcot Marie Tooth 2B Peripheral Sensory Neuropathy. *Commun Biol.* 2022;5(1):717. doi: 10.1038/s42003-022-03632-1. PMID: 35851620; PMCID: PMC9293960.

[12] Gomez Godinez V, Morar V, Carmona C, Gu Y, Sung K, Shi LZ, Wu C, Preece D, Berns MW. Laser-Induced Shockwave (LIS) to Study Neuronal Ca2+ Responses. *Front Bioeng Biotechnol.* 2021;9:598896. doi: 10.3389/fbioe.2021.598896. PMID: 33681154; PMCID: PMC7928400.

[13] Zhou J, Tian F, Hu J, Shi ZL, Godinez VG, Tsai DP, Liu Z. Eagle-Eye Inspired Meta-Device for Phase Imaging. *Adv Mater.* 2024;36(32):e2402751. doi: 10.1002/adma.202402751. PMID: 38816897.

[14] Pan Y, Shi LZ, Yoon CW, Preece D, Gomez-Godinez V, Lu S, Carmona C, Woo SH, Chien S, Berns MW, Liu L, Wang Y. Mechanosensor Piezo1 mediates bimodal patterns of intracellular calcium and FAK signaling. *EMBO J.* 2022;41(17):e111799. doi: 10.15252/embj.2022111799. PMID: 35844093; PMCID: PMC9433934.

[15] Gu Y, Pope A, Smith C, Carmona C, Johnstone A, Shi L, Chen X, Santos S, Bacon-Brenes CC, Shoff T, Kleczko KM, Frydman J, Thompson LM, Mobley WC, Wu C. BDNF and TRiC-inspired reagent rescue cortical synaptic deficits in a mouse model of Huntington's disease. *Neurobiol Dis.* 2024;195:106502. doi: 10.1016/j.nbd.2024.106502. PMID: 38608784; PMCID: PMC11890210.

[16] Stilgoe AB, Favre-Bulle IA, Watson ML, Gomez-Godinez V, Berns MW, Preece D, Rubinsztein-Dunlop H. Shining Light in Mechanobiology: Optical Tweezers, Scissors, and Beyond. *ACS Photonics.* 2024;11(3):917-940. doi: 10.1021/acsphotonics.4c00064. PMID: 38523746; PMCID: PMC10958612.

[17] Wang H, Li S, Zhang H, Wang Y, Hao S, Wu X. BLM prevents instability of structure-forming DNA sequences at common fragile sites. *PLoS Genet.* 2018;14(11):e1007816. doi: 10.1371/journal.pgen.1007816. PMID: 30496191; PMCID: PMC6289451.